Rigidity-Based Multiagent Layered Formation Control

Saba Ramazani, *Student Member, IEEE*, Rastko Selmic, *Senior Member, IEEE*, and Marcio de Queiroz, *Member, IEEE*

***Abstract*—This paper provides a solution to the nonplanar multiagent formation control problem using graph rigidity. We consider a 3-D multiagent formation control where multiple agents are operating in one plane and some other agents are operating outside of that plane. This can be referred to as a layered formation control where the objective is for all agents to cooperatively acquire a predefined formation shape using a decentralized control law. The proposed control strategy is based on regulating the interagent distances. A rigorous stability analysis is presented that guarantees convergence of these distances to desired values. Simulation results are presented to support the theoretical results.**

***Index Terms*—Formation control, Lyapunov stability, multiagent control, rigid graphs.**

I. Introduction

THE TOPIC of cooperative formation control of multiagent systems has been of particular interest in recent years. A multiagent system refers to a team of interacting agents that together perform a complex task [1]. Behavior similar to that of multiagent systems has existed in nature for a long time. The collective behavior of groups of birds, bees, and fish has granted them the ability to perform complex functions that cannot be achieved by individual members of the group [2]. The behavior of these biological multiagent systems, as demonstrated in nature, is distributed and decentralized. Each individual member of the group has its own local sensing and control mechanisms without global knowledge or planning. This multiagent system behavior is also demonstrated in engineering applications by teams of autonomous unmanned aerial vehicles (UAVs), unmanned ground vehicles (UGVs), and unmanned underwater vehicles (UUVs) that are deployed to perform surveillance, reconnaissance, and search of an area [1], [3], [4].

Manuscript received April 16, 2015; revised November 3, 2015 and March 16, 2016; accepted April 27, 2016. This work was supported by the NASA under grant #NNX15AH82H and Louisiana Space Consortium under grant LEQSF(2015-2018)-LaSPACE. This paper was recommended by Associate Editor J. Su.

S. Ramazani and R. Selmic are with the Department of Electrical Engineering, Louisiana Tech University, Ruston, LA 71272 USA (e-mail: sra028@latech.edu; rselmic@latech.edu).

M. de Queiroz is with the Department of Mechanical and Industrial Engineering, Louisiana State University, Baton Rouge, LA 70803 USA (e-mail: mdeque1@lsu.edu).

Color versions of one or more of the figures in this paper are available online at http://ieeexplore.ieee.org.

Digital Object Identifier 10.1109/TCYB.2016.2568164

In a formation-type behavior, the group of agents move together from one point to another to perform a task while maintaining the original formation structure. This structure is a geometric shape, and maintaining this shape implies that the formation at one instant of time is congruent to the formation at another instant of time. Such behavior is also displayed in nature by flocks of birds and schools of fish [5].

Rigid graph theory [6], [7] plays a crucial role in analyzing the multiagent formation shape and describing the information architecture of the system. In this case, the rigidity matrix is important for the stability analysis of the formation control. Some previous work that used rigid graph theory to address the multiagent formation problem can be found in [5] and [8]–[10].

The formation control problems are generally categorized based on position, displacement, and interagent distances. In the distance-based control, the agents sense the relative position of their neighboring agents, using onboard sensors, with respect to their own local coordinate systems. Therefore, a main advantage of this control, compared to position- and displacement-based formation control, is that less global information is needed by the agents [11]. This is especially useful in global positioning system-denied environments where unmanned multiagent systems are used for search and rescue operations, planetary explorations, indoor/outdoor navigation, and target tracking.

Most of the available distance-based formation control results in the literature use the single integrator model for the agents' motion in the plane [12]–[17]. In this paper, in addition to the single integrator agent model, we also present the more realistic and practical [18] formation control of agents modeled as double integrators. Another contribution of this paper is to provide a theoretical framework for real world applications which are often in 3-D space as opposed to the plane. Recently, some work has been done to extend the multiagent formations to 3-D space [9], [19]. As opposed to the control approach presented in [19] for a 3-D tetrahedral formation with only four agents, there is no limit in our work for the number of agents. The control of rigid formations in 3-D using single and double integrator models is considered in [9]. Our approach differs in that we consider the infinitesimally and minimally rigid 3-D formations. In this case, minimally rigid refers to multiagent formations with minimum number of communication and control links between the agents. The previous work [20] addressed the formation acquisition of n agents in the plane. In this paper, we extend the results in [20] to 3-D

This article has been accepted for inclusion in a future issue of this journal. Content is final as presented, with the exception of pagination.

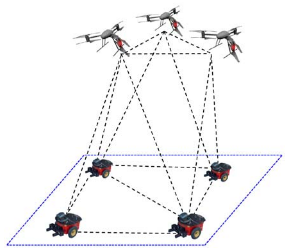

Fig. 1. Formation control concept under the layered sensing framework.

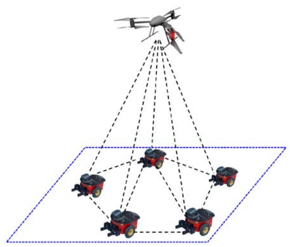

Fig. 2. Formation control concept under the coning framework.

space and provide stability analysis and sufficient conditions for the initial conditions that guarantees the convergence of the agents' formation to the desired framework.

We consider a nonhierarchical formation structure where there is no leader–follower in the formation. No hierarchy allows a balanced task distribution among the agents and is expected to be more robust to atmospheric disturbances and variations in the speed of the individual agents [21].

The concepts of layered sensing and formation control are combined in this paper to address the multiagent layered formation control problem. Layered sensing was first introduced by the U.S. Air Force Research Laboratory and it refers to the appropriate combination of sensors/platforms, infrastructure, and exploitation capabilities that generate situational awareness and directly supports "tailored effects" [22]. An example of combined layered sensing and formation control scenario is shown in Fig. 1 and includes UGVs and UAVs. The upper layer agents can be with or without sensors for the ground supporting mission.

In this paper we address the layered formation control of n lower layer agents that belong to a plane Q, modeled by an undirected graph and r upper layer agents that are moving outside of the plane Q, as shown in Fig. 1. Triangulation of the layered formation is proposed to obtain an infinitesimally and minimally rigid framework in 3-D space.

As a special case, the layered formation control with one agent in the upper layer (i.e., $r = 1$) is also addressed (see Fig. 2). Here we use the concept of coning [23], [24] to create a 3-D formation that retains the properties of infinitesimal and minimal rigidity of the framework for the lower layer agents in plane Q.

II. Preliminaries

The formation shape of a multiagent system is represented by an undirected graph $G = (V, E)$ where $V = (1, 2, \ldots, n)$ is the vertex set of this graph that represents the agents and E is the edge set that represents the communication links between the agents. The number of vertices and edges of G are denoted by $|V|$ and $|E|$, respectively.

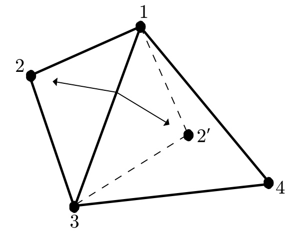

Fig. 3. Noncongruent framework that depicts flip ambiguity [vertex 2 can be flipped over the edge (1, 3) to the symmetric position 2′].

A framework is a realization of a graph at given points in $\mathbb{R}^d$ where $d \in \{2, 3\}$. A d-dimensional framework F is a pair (G, p) where $p = (p_1, \ldots, p_n) \in \mathbb{R}^{dn}$ and $p_i \in \mathbb{R}^d$ is the coordinate of vertex i [20]. Given an arbitrary ordering of the edges of G, an edge function $\Phi_G : \mathbb{R}^{dn} \to \mathbb{R}^{|E|}$ associated with (G, p) is given by

$$\Phi_G(p) = \left(\ldots, \left\|p_i - p_j\right\|^2, \ldots\right), (i, j) \in E \tag{1}$$

where $\|\cdot\|$ denotes the Euclidean norm. The rigidity matrix $R(p) : \mathbb{R}^{dn} \to \mathbb{R}^{|E|\times dn}$ of (G, p) is defined as

$$R(p) = \frac{1}{2}\frac{\partial \Phi_G(p)}{\partial p}. \tag{2}$$

Two frameworks (G, p) and (G, q) are equivalent if $\Phi_G(p) = \Phi_G(q)$ and are congruent if $\|p_i - p_j\| = \|q_i - q_j\|$ for all $i, j \in V$ [20], [25]. In the case where two frameworks are equivalent but not congruent, then they are flip ambiguous [2]. The notion of flip ambiguity is illustrated in Fig. 3.

In order to determine the rigidity of a formation, both number of the edges and their distribution among the graph vertices matter. Laman's theorem is known to be a key result that is used in solving the rigidity-based formation control problems in 2-D.

Theorem 1 [26]: A graph $G = (V, E)$ modeling a formation in 2-D is rigid if and only if there exists a subgraph $G' = (V, E')$, $E' \subset E$ with $|E'| = 2|V| - 3$ such that for any $V' \subset V$, the associated induced subgraph $G'' = (V', E'')$ of G' with $E'' \subset E'$, satisfies $|E''| \le 2|V'| - 3$.

A graph is minimally rigid if it is rigid and if no single edge can be removed from the graph without causing the graph to lose its rigidity [27]. A graph $G = (V, E)$ is minimally rigid in 2-D or 3-D if and only if $|E| = 2|V| - 3$ or $|E| = 3|V| - 6$, respectively [2], [28].

A framework (G, p) where $n > d$ and p is generic (the affine span of p is all of R^d) is infinitesimally rigid if and only if $\text{rank}[R(p)] = dn - \binom{d+1}{2}$. Therefore, (G, p) is flexible if $|E| < dn - \binom{d+1}{2}$ [6], [29], [30].

Lemma 1: If the framework $F = (G, p)$ is infinitesimally and minimally rigid in 3-D, then $R(p)R^T(p)$ is invertible.

Proof: We know that if F is infinitesimally and minimally rigid in 3-D, then $\text{rank}[R(p)] = 3|V| - 6$ and $|E| = 3|V| - 6$. Therefore, $R(p)$ has full row rank. Since, $R^T(p)$ has full column rank and $\text{rank}[R(p)] = \text{rank}[R(p)R^T(p)]$, then $R(p)R^T(p) \in \mathbb{R}^{|E|\times|E|}$ is invertible. ■

Remark 1: The rigidity matrix $R(p)$ for the framework F is constructed with an arbitrary ordering of vertices and edges and has $3|V|$ columns and $|E|$ rows. The rows of $R(p)$ correspond to the edges of G. If there is an edge between vertices i and j then the entries $x_{l_i} - x_{l_j}$, $y_{l_i} - y_{l_j}$, $z_{l_i} - z_{l_j}$, $x_{l_j} - x_{l_i}$, $y_{l_j} - y_{l_i}$, and $z_{l_j} - z_{l_i}$ will fill columns $3i-2$, $3i-1$, $3i$, $3j-2$, $3j-1$, and $3j$ of $R(p)$, respectively. The entries of the other columns will be zero.

A surface in $\mathbb{R}^3$ is triangulated if it is covered with a collection of triangles and if any two triangles intersect, their intersection is a common edge or vertex [31]. A graph $G = (V, E)$ is polyhedral if and only if there exists $p = (p_1, \ldots, p_n) \in \mathbb{R}^{3|V|}$ such that $p_i \neq p_j$ for $i \neq j$ and $(i, j) \in E$ are the edges of a convex polyhedron in $\mathbb{R}^3$ [32]. A triangulated convex polyhedral surface with vertices only in the natural edges, is infinitesimally rigid. The natural edges are 1-D intersections of a support plane with the convex polyhedral surface [33].

Coning is a technique in rigidity which takes frameworks in $\mathbb{R}^N$ where $N \in \{1, 2, 3, \ldots\}$ to frameworks in $\mathbb{R}^{N+1}$ while preserving first-order rigidity (or infinitesimal rigidity) [23], [24]. A graph $G = (V, E)$ is coned by adding a new vertex c, and adding edges from this vertex to all the original vertices in G. This will create the cone graph $G * \{c\}$ with $V(G * \{c\}) = V(G) \cup \{c\}$ where the cone vertex c is distinct from the vertices of G. If p_c is a configuration for $G * \{c\}$ and $H \cong \mathbb{R}^N$ is a hyperplane, then we denote p_H to be the projection of p_c from the cone vertex into H. We call p_c and p_H a projection pair of configurations.

A general version of the infinitesimal rigidity coning theorem is presented in [24] and its proof can be found in [23]. The following lemma is directed toward the cone framework (one upper layer agent in the framework) of interest in this paper.

Lemma 2 [23]: Let G be a graph that represents a group of n agents in $\mathbb{R}^2$, $G * \{c\}$ be the cone graph with cone vertex c representing the upper layer agent, and p^* and p_H be a projection pair of configurations. Then $(G * \{c\}, p^*)$ is infinitesimally rigid in $\mathbb{R}^3$ if and only if (G, p_H) is infinitesimally rigid in $\mathbb{R}^2$.

III. Problem Formulation

In this paper, it is assumed that agents are equipped with sensors such as ultrasonic or infrared-based relative positioning sensors [34] that allow them to measure the distance and direction between selected agents.

A. Nonplanar Multiagent Layered Formation Control With Single Integrator Model

Consider a system of n agents in the plane Q and r agents in an upper layer outside of the plane Q, modeled by the single integrator (model $\mathcal{W}_1$) [1], [13], [14], [35]

$$\mathcal{W}_1 : \dot{p}_{l_i} = u_{l_i}, i = 1, \ldots, n, n+1, \ldots, n+r \tag{3}$$

where $p_{l_i} = (x_{l_i}, y_{l_i}, 0) \in \mathbb{R}^3$ for $i = 1, \ldots, n$ is the location of the i-th agent in local coordinates in plane Q that is defined by $z = 0$.

The location of the upper layer agents is defined by $p_{l_i} = (x_{l_i}, y_{l_i}, z_{l_i}) \in \mathbb{R}^3$ for $i = n+1, \ldots, n+r$, where z_{l_i} is the distance of the agents from plane Q. The control input for the ith agent in plane Q and the upper layer agents is $u_{l_i} \in \mathbb{R}^3$ for $i = 1, \ldots, n, n+1, \ldots, n+r$.

Consider a formation in $\mathbb{R}^3$ that can be triangulated for the layered system mentioned above described by the framework $F_l^* = (G_l^*, p_l^*)$ where $G_l^* = (V_l, E_l)$ and $p_l^* = (p_{l_1}^*, \ldots, p_{l_n}^*, p_{l_{n+1}}^*, \ldots, p_{l_{n+r}}^*)$. Let F_l^* represent the desired layered formation of the system of $n + r$ agents.

Given the actual formation $F_l(t) = (G_l^*, p_l(t))$ where $p_l = (p_{l_1}, \ldots, p_{l_n}, p_{l_{n+1}}, \ldots, p_{l_{n+r}})$ and assuming that at $t = 0$, $\|p_{l_i}(0) - p_{l_j}(0)\| \neq d_{l_{ij}}$ for $(i, j) \in E_l$, where $d_{l_{ij}} = \|p_{l_i}^* - p_{l_j}^*\| > 0$ is the constant desired distance between agents i and j in the layered formation, the control objective is to design the control input u_{l_i} such that

$$\left\|p_{l_i}(t) - p_{l_j}(t)\right\| \to d_{l_{ij}} \text{ as } t \to \infty, (i, j) \in E_l. \tag{4}$$

B. Nonplanar Multiagent Layered Formation Control With Double Integrator Model

In this section, the problem of nonplanar multiagent layered formation control is formulated using the double integrator model [20], [36], [37].

Given a system of n agents in the plane Q and r agents in an upper layer outside of the plane Q, modeled by the double integrator (model $\mathcal{W}_2$)

$$\mathcal{W}_2 : \begin{cases} \dot{p}_{l_i} = v_{l_i} \\ \dot{v}_{l_i} = u_{l_i}, \quad i = 1, \ldots, n, n+1, \ldots, n+r \end{cases} \tag{5}$$

where $v_{l_i} \in \mathbb{R}^3$ for $i = 1, \ldots, n, n+1, \ldots, n+r$ is the velocity and u_{l_i} is the acceleration-level control input for the i-th agent. The control objective is to design the control input u_{l_i} such that (4) is satisfied.

IV. Control Algorithms

We extend the results from [20] to solve the formation acquisition and stabilization problem in 3-D where the upper layer agents are operating outside of the plane defined by the lower layer agents.

A. Single Integrator Model

Define the relative position of two agents in the layered formation as

$$\tilde{p}_{l_{ij}} = p_{l_i} - p_{l_j}, (i, j) \in E_l. \tag{6}$$

The distance error for the group of $n + r$ agents and the corresponding distance error dynamics are given by

$$e_{l_{ij}} = \left\|\tilde{p}_{l_{ij}}\right\| - d_{l_{ij}} \tag{7}$$

$$\begin{aligned} \dot{e}_{l_{ij}} &= \frac{d}{dt}\sqrt{\tilde{p}_{l_{ij}}^T \tilde{p}_{l_{ij}}} = \left(\tilde{p}_{l_{ij}}^T \tilde{p}_{l_{ij}}\right)^{-\frac{1}{2}} \tilde{p}_{l_{ij}}^T \left(u_{l_i} - u_{l_j}\right) \\ &= \frac{\tilde{p}_{l_{ij}}^T \left(u_{l_i} - u_{l_j}\right)}{e_{l_{ij}} + d_{l_{ij}}}. \end{aligned} \tag{8}$$

For control algorithm development and stability analysis, consider the potential function [13], [14], [20]

$$M_{ij} = \frac{1}{4} e_{l_{ij}}^2 \left(e_{l_{ij}} + 2d_{l_{ij}}\right)^2 \tag{9}$$

where M_{ij} is positive definite and radially unbounded in $e_{l_{ij}}$. Define

$$M(e_l) = \sum_{(i,j)\in E_l} M_{ij}\left(e_{l_{ij}}\right) \tag{10}$$

where $M_{ij}(e_{l_{ij}})$ was given in (9). The time derivative of (10) is then given by

$$\dot{M} = \sum_{(i,j)\in E_l} \frac{\partial M_{ij}}{\partial e_{l_{ij}}} \frac{\tilde{p}_{l_{ij}}^T \left(u_{l_i} - u_{l_j}\right)}{e_{l_{ij}} + d_{l_{ij}}}. \tag{11}$$

As shown in [20], it follows from (1), (2), (7), and (8) that (11) can be expressed as:

$$\dot{M} = \beta^T(e_l) R(p_l) u_l \tag{12}$$

where $u_l = (u_{l_1}, \ldots, u_{l_n}, u_{l_{n+1}}, \ldots, u_{l_{n+r}}) \in \mathbb{R}^{3(n+r)}$, $R(p_l) \in \mathbb{R}^{|E_l|\times 3(n+r)}$, $e_l = (\ldots, e_{l_{ij}}, \ldots) \in \mathbb{R}^{|E_l|}$, and

$$\begin{aligned}\beta(e_l) &= \left(\ldots, \frac{\frac{\partial M_{ij}}{\partial e_{l_{ij}}}}{e_{l_{ij}} + d_{l_{ij}}}, \ldots\right) \\ &= \left(\ldots, e_{l_{ij}}\left(e_{l_{ij}} + 2d_{l_{ij}}\right), \ldots\right), (i,j) \in E_l.\end{aligned} \tag{13}$$

The terms in e_l and $\beta(e_l) \in \mathbb{R}^{|E_l|}$ are ordered the same way as in (1).

The following theorem relates the triangulation of the layered framework in 3-D space and the infinitesimal and minimal rigidity of the formation.

Theorem 2 [33]: Let $F_l^* = (G_l^*, p_l^*)$, which consists of n agents in the plane Q and r upper layer agents, be the desired framework for a layered formation in $\mathbb{R}^3$. If the surface of F_l^* is arbitrarily triangulated, then the layered formation F_l^* is infinitesimally and minimally rigid in $\mathbb{R}^3$.

The proof for infinitesimal rigidity of the framework F_l^* in Theorem 2 is presented in [33] and [38]. Such a framework has $|E_l| = 3|V_l| - 6$ edges and therefore is minimally rigid in 3-D [2], [28].

Corollary 1 [20]: Define the function

$$\Omega\left(F_l, F_l^*\right) = \sum_{(i,j)\in E_l} \left(\left\|p_{l_i} - p_{l_j}\right\| - \left\|p_{l_i}^* - p_{l_j}^*\right\|\right)^2. \tag{14}$$

If F_l^* is infinitesimally rigid and $\Omega(F_l, F_l^*) \le \varepsilon$ where ε is a sufficiently small positive constant, then F_l is also infinitesimally rigid.

The following theorem shows that the control law [20]:

$$u_l = -k_c R^T(p_l)\beta(e_l) \tag{15}$$

where k_c is a positive control gain, achieves the local asymptotic stability of the desired layered formation $F_l^* = (G_l^*, p_l^*)$. Note that from (1), the rigidity matrix function R is dependent on $\tilde{p}_l$ but in this paper the argument of this function will be given as p_l.

Theorem 3: Given a group of n lower layer agents and $r \ge 1$ upper layer agents with a layered formation $F_l(t) = (G_l^*, p_l(t))$ in $\mathbb{R}^3$ and modeled by $\mathcal{W}_1$, let δ be a small positive constant and $\tilde{p}_l(0)$, where $\tilde{p}_l = (\ldots, \tilde{p}_{ij}, \ldots) \in \mathbb{R}^{3|E_l|}$, is the initial condition. If $\tilde{p}_l(0) \in \mathcal{S}_1$ where

$$\mathcal{S}_1 = \left\{\tilde{p}_l \in \mathbb{R}^{3|E_l|} \middle| \left|\left\|\tilde{p}_{l_{ij}}\right\|^2 - d_{l_{ij}}^2\right| \le \frac{2\sqrt{\delta}}{\sqrt{|E_l|}}, (i,j) \in E_l\right\} \tag{16}$$

then $F_l(t)$ is infinitesimally and minimally rigid and the control law (15) achieves the local asymptotic stability of the desired formation F_l^* ensuring $\|p_{l_i}(t) - p_{l_j}(t)\| \to d_{l_{ij}}$ as $t \to \infty$ for all $(i,j) \in E_l$.

Proof: Theorem 2 ensures the infinitesimal and minimal rigidity of the layered formation F_l^* in 3-D. Since F_l^* is minimally rigid and has the same number of edges as $F_l(t)$, we know that $F_l(t)$ is also minimally rigid for all time. Note that (10) can be written as

$$\begin{aligned}M(e_l) &= \frac{1}{4}\sum_{(i,j)\in E_l}\left[\left(\left\|\tilde{p}_{l_{ij}}\right\| - d_{l_{ij}}\right)^2\left(\left\|\tilde{p}_{l_{ij}}\right\| + d_{l_{ij}}\right)^2\right] \\ &= \frac{1}{4}\sum_{(i,j)\in E_l}\left(\left\|\tilde{p}_{l_{ij}}\right\|^2 - d_{l_{ij}}^2\right)^2.\end{aligned} \tag{17}$$

Condition $M(e_l) \le \delta$ is equivalent to

$$\sum_{(i,j)\in E_l}\left(\left\|\tilde{p}_{l_{ij}}\right\|^2 - d_{l_{ij}}^2\right)^2 \le 4\delta. \tag{18}$$

A sufficient condition for (18) is given by

$$\left|\left\|\tilde{p}_{l_{ij}}\right\|^2 - d_{l_{ij}}^2\right| \le \frac{2\sqrt{\delta}}{\sqrt{|E_l|}}, (i,j) \in E_l. \tag{19}$$

Therefore $\tilde{p}_l \in \mathcal{S}_1$ implies $M(e_l) \le \delta$ (valid for all $t > 0$). Reference [20, Lemma 2] establishes the equivalence between $M(e_l) \le \delta$ and $\Omega(F_l, F_l^*) \le \varepsilon$ and since F_l^* is infinitesimally rigid, Corollary 1 shows that the formation F_l is also infinitesimally rigid for $\tilde{p}_l \in \mathcal{S}_1$. Therefore, according to Lemma 1, $R(p_l)R^T(p_l)$ is invertible for $\tilde{p}_l \in \mathcal{S}_1$.

Substituting (15) into (12) yields

$$\dot{M} = -k_c \beta^T(e_l) R(p_l) R^T(p_l) \beta(e_l). \tag{20}$$

Therefore

$$\dot{M} \le -k_c \lambda_{\min}\left(R(p_l)R^T(p_l)\right) L(e_l) \text{ for } \tilde{p}_l(t) \in \mathcal{S}_1 \tag{21}$$

where $\lambda_{\min}(\cdot)$ denotes the minimum eigenvalue and $L(e_l) = \beta^T(e_l)\beta(e_l)$. It follows from the negative definiteness of (20) that the level sets of M are invariant [39] for $\tilde{p}_l(0) \in \mathcal{S}_1$ and $e_l = 0$ is asymptotically stable for $\tilde{p}_l(0) \in \mathcal{S}_1$. Therefore, $\|p_{l_i}(t) - p_{l_j}(t)\| \to d_{l_{ij}}$ as $t \to \infty$ for all $(i,j) \in E_l$ and the control law (15) achieves the local asymptotic stability of the desired formation $F_l^* = (G_l^*, p_l^*)$. ■

Remark 2: Note that Theorem 3 provides a control law for local asymptotic stability of the formation and sufficient conditions for the set of allowed initial conditions $\mathcal{S}_1$ that guarantees the convergence to the desired formation. This result establishes a region for local asymptotic stability, but it does not show how to determine such region. That is, it is an existence result, rather than a constructive result, with respect to the stability region. The value of δ can be found by trial-and-error only.

Remark 3: The control (15) can be expressed componentwise as

$$u_{l_i} = -k_c \sum_{j \in \Psi_i} \tilde{p}_{l_{ij}} e_{l_{ij}} \left(e_{l_{ij}} + 2d_{l_{ij}} \right) \tag{22}$$

where $\Psi_i(E_l) = \{j \in V_l | (i, j) \in E_l\}$ is a set of all neighboring vertices to vertex (agent) i in graph G_l^*. It is easy to see from (22) that the developed control is decentralized in the sense that the control input for each agent is only dependent on the relative position and velocity of the neighboring agents in the formation and agents' own absolute velocity.

The following lemma uses the absolute initial and desired positions of the agents and shows that (15) achieves the local asymptotic stability of the desired formation F_l^*. Therefore, Lemma 3 establishes the conditions that prevent convergence to ambiguous formations.

Lemma 3: Given model $\mathcal{W}_1$, let δ be a small positive constant and $p_l(0) \in \mathbb{R}^{3(n+r)}$ is the initial condition. If $p_l(0) \in \mathcal{S}_2$ where

$$\mathcal{S}_2 = \left\{ p_l \in \mathbb{R}^{3(n+r)} \middle| \max_{i \in V_l} \left\| p_{l_i} - p_{l_i}^* \right\| + D_l \le \sqrt[4]{\frac{\delta}{4|E_l|}} \right\} \tag{23}$$

and $D_l = \max(d_{l_{ij}})$, then the control law (15) achieves the local asymptotic stability of the desired formation F_l^* and ensures $\|p_{l_i}(t) - p_{l_j}(t)\| \to d_{l_{ij}}$ as $t \to \infty$ for all $(i, j) \in E_l$.

Proof: A sufficient condition for (19) is

$$\max_{(i,j)\in E_l} \left| \left\| p_{l_i} - p_{l_j} \right\| - d_{l_{ij}} \right| \max_{(i,j)\in E_l} \left(\left\| p_{l_i} - p_{l_j} \right\| + d_{l_{ij}} \right) \le \frac{2\sqrt{\delta}}{\sqrt{|E_l|}}. \tag{24}$$

Using inequality

$$\left\| p_{l_i} - p_{l_j} \right\| \le \left\| p_{l_i} - p_{l_i}^* \right\| + \left\| p_{l_j} - p_{l_j}^* \right\| + d_{l_{ij}} \tag{25}$$

a sufficient condition for (24) is

$$\max_{(i,j)\in E_l} \left(\left\| p_{l_i} - p_{l_i}^* \right\| + \left\| p_{l_j} - p_{l_j}^* \right\| \right) \max_{(i,j)\in E_l} \left(\left\| p_{l_i} - p_{l_i}^* \right\| + \left\| p_{l_j} - p_{l_j}^* \right\| + 2d_{l_{ij}} \right) \le \frac{2\sqrt{\delta}}{\sqrt{|E_l|}}. \tag{26}$$

A sufficient condition for (26) is given by

$$\max_{i \in V_l} \left\| p_{l_i} - p_{l_i}^* \right\| + D_l \le \sqrt[4]{\frac{\delta}{4|E_l|}}. \tag{27}$$

Using Theorem 3, it follows that $\|p_{l_i}(t) - p_{l_j}(t)\| \to d_{l_{ij}}$ as $t \to \infty$ for all $(i, j) \in E_l$ and the control law (15) achieves the local asymptotic stability of the desired formation $F_l^* = (G_l^*, p_l^*)$. ■

Remark 4: Note that Lemma 3 provides sufficient conditions for the formation convergence to the desired formation in terms of initial positions of each agent. An upper bound of the norm of initial position error for each agent is given by (27). Conservatism of the bound (27) depends on uniformity of distances $d_{l_{ij}}$, i.e., more uniform distances will cause a less conservative bound.

Remark 5: The system of n agents in the plane Q and a single upper layer agent outside of the plane Q is considered a special case for nonplanar multiagent layered formation control with single [40] and double integrator models. The triangulation method still applies and is referred to as coning which allows for retaining the infinitesimal and minimal rigidity of the n planar agents in 3-D space.

Note that the control algorithms in this section are applicable to a cone framework. In such a framework, the coning method (Lemma 2) ensures that the layered formation $F_l^*(t) = (G_l^*, p_l^*(t))$ is infinitesimally rigid in $\mathbb{R}^3$ [40]. Since the cone framework is triangulated and has $|E_l| = 3|V_l| - 6$ edges, F_l^* is also minimally rigid in 3-D.

B. Double Integrator Model

Define the relative position of two agents as in (6). The distance error for the group of n lower layer agents and r upper layer agents is defined in (7) and distance error dynamics are given by

$$\dot{e}_{l_{ij}} = \frac{\tilde{p}_{l_{ij}}^T \left(v_{l_i} - v_{l_j} \right)}{e_{l_{ij}} + d_{l_{ij}}} \tag{28}$$

where (5) was used. Consider the potential function in (9). Let

$$M_1(e_l) = \sum_{(i,j)\in E_l} M_{ij}\left(e_{l_{ij}}\right). \tag{29}$$

The time derivative of (29) along (28) is given by

$$\dot{M}_1 = \sum_{(i,j)\in E_l} \frac{\partial M_{ij}}{\partial e_{l_{ij}}} \frac{\tilde{p}_{l_{ij}}^T \left(v_{l_i} - v_{l_j} \right)}{e_{l_{ij}} + d_{l_{ij}}}. \tag{30}$$

It follows from (1), (2), and (7) that (30) can be written as:

$$\dot{M}_1 = \beta^T(e_l) R(p_l) v_l \tag{31}$$

where $v_l = (v_{l_1}, \ldots, v_{l_n}, v_{l_{n+1}}, \ldots, v_{l_{n+r}}) \in \mathbb{R}^{3(n+r)}$.

Using the backstepping method [20], [41], consider the variable $s_l = (s_{l_1}, \ldots, s_{l_n}, s_{l_{n+1}}, \ldots, s_{l_{n+r}}) \in \mathbb{R}^{3(n+r)}$ defined as

$$s_l = v_l - f_l \tag{32}$$

where $f_l = (f_{l_1}, \ldots, f_{l_n}, f_{l_{n+1}}, \ldots, f_{l_{n+r}}) \in \mathbb{R}^{3(n+r)}$ is a virtual velocity input for the layered formation that is given by

$$f_l = -k_v R^T(p_l) \beta(e_l) \tag{33}$$

and k_v is a positive constant. Define the total potential function

$$M_2(e_l, s_l) = M_1(e_l) + \frac{1}{2} s_l^T s_l. \tag{34}$$

Taking the time derivative of (34) and using (5), (31), and (32) yields

$$\begin{aligned} \dot{M}_2 &= \beta^T(e_l) R(p_l) v_l + s_l^T \dot{s}_l \\ &= \beta^T(e_l) R(p_l) f_l + s_l^T \left[u_l + R^T(p_l) \beta(e_l) - \dot{f}_l \right] \end{aligned} \tag{35}$$

where $\dot{f}_l = -k_v(\dot{R}^T(p_l)\beta(e_l) + R^T(p_l)\dot{\beta}(e_l))$ and $u_l = (u_{l_1}, \ldots, u_{l_n}, u_{l_{n+1}}, \ldots, u_{l_{n+r}}) \in \mathbb{R}^{3(n+r)}$ is the control input for the layered formation.

The following theorem shows that the control law [20]:

$$u_l = -k_a s_l + \dot{f}_l - R^T(p_l) \beta(e_l), \tag{36}$$

where k_a is a positive control gain, achieves the asymptotic stability of the desired layered formation $F_l^* = (G_l^*, p_l^*)$.

Theorem 4: Given a group of n lower layer agents and $r \geq 1$ upper layer agents with a layered formation $F_l(t) = (G_l^*, p_l(t))$ in $\mathbb{R}^3$ and modeled by $\mathcal{W}_2$, let δ be a positive constant and $\tilde{p}_l(0) \in \mathbb{R}^{3|E_l|}$ and $v_l(0) \in \mathbb{R}^{3(n+r)}$ are the initial conditions. If $(\tilde{p}_l(0), v_l(0)) \in \mathcal{T}_1$ where

$$\mathcal{T}_1 = \Bigg\{ (\tilde{p}_l, v_l) \in \mathbb{R}^{3|E_l|} \times \mathbb{R}^{3(n+r)} \Bigg| \frac{1}{2}|E_l| \max_{(i,j)\in E_l} \left(\left\|\tilde{p}_{l_{ij}}\right\|^2 - d_{l_{ij}}^2 \right)^2 + |V_l| \max_{i \in V_l} \left(\left\|v_{l_i}\right\| + k_v |\Psi_i| \max_{j \in \Psi_i} \left\|\tilde{p}_{l_{ij}}\right\|^3 \right)^2 \leq 2\delta \Bigg\} \quad (37)$$

then $F_l(t)$ is infinitesimally and minimally rigid and the control law (36) achieves the asymptotic stability of the desired formation F_l^* and ensures $\|p_{l_i}(t) - p_{l_j}(t)\| \to d_{l_{ij}}$ as $t \to \infty$ for all $(i, j) \in E_l$.

Proof: Note that (34) can be written as

$$M_2(e_l, s_l) = \frac{1}{4} \sum_{(i,j)\in E_l} \left(\left\|\tilde{p}_{l_{ij}}\right\|^2 - d_{l_{ij}}^2 \right)^2 + \frac{1}{2} \sum_{i \in V_l} \left\|s_{l_i}\right\|^2. \quad (38)$$

Condition $M_2(e_l, s_l) \leq \delta$ is equivalent to

$$\frac{1}{2} \sum_{(i,j)\in E_l} \left(\left\|\tilde{p}_{l_{ij}}\right\|^2 - d_{l_{ij}}^2 \right)^2 + \sum_{i \in V_l} \left\|s_{l_i}\right\|^2 \leq 2\delta. \quad (39)$$

Substituting (32) into (39) and knowing that

$$f_{l_i} = -k_v \sum_{j \in \Psi_i} \tilde{p}_{l_{ij}} e_{l_{ij}} \left(e_{l_{ij}} + 2d_{l_{ij}}\right), \quad (40)$$

a sufficient condition for (39) is

$$\frac{1}{2}|E_l| \max_{(i,j)\in E_l} \left(\left\|\tilde{p}_{l_{ij}}\right\|^2 - d_{l_{ij}}^2 \right)^2 + |V_l| \max_{i \in V_l} \left\| v_{l_i} + k_v \sum_{j \in \Psi_i} \tilde{p}_{l_{ij}} e_{l_{ij}} \left(e_{l_{ij}} + 2d_{l_{ij}}\right) \right\|^2 \leq 2\delta. \quad (41)$$

Using the triangle inequality, the sufficient condition is given by

$$\frac{1}{2}|E_l| \max_{(i,j)\in E_l} \left(\left\|\tilde{p}_{l_{ij}}\right\|^2 - d_{l_{ij}}^2 \right)^2 + |V_l| \max_{i \in V_l} \left(\left\|v_{l_i}\right\| + k_v \sum_{j \in \Psi_i} \left\|\tilde{p}_{l_{ij}}\right\| \left(\left\|\tilde{p}_{l_{ij}}\right\|^2 - d_{l_{ij}}^2 \right) \right)^2 \leq 2\delta. \quad (42)$$

$$\frac{1}{2}|E_l| \max_{(i,j)\in E_l} \left(\left\|\tilde{p}_{l_{ij}}\right\|^2 - d_{l_{ij}}^2 \right)^2 + |V_l| \max_{i \in V_l} \left(\left\|v_{l_i}\right\| + k_v |\Psi_i| \max_{j \in \Psi_i} \left\|\tilde{p}_{l_{ij}}\right\|^3 \right)^2 \leq 2\delta. \quad (43)$$

Therefore $(\tilde{p}_l(t), v_l(t)) \in \mathcal{T}_1$ implies $M_2(e_l, s_l) \leq \delta$ (valid for all $t > 0$). Reference [20, Lemma 2] establishes the equivalence between $M_1(e_l) \leq \delta$ and $\Omega(F_l, F_l^*) \leq \varepsilon$ and since F_l^* is infinitesimally rigid, Corollary 1 shows that the formation F_l is also infinitesimally rigid for $(\tilde{p}_l(t), v_l(t)) \in \mathcal{T}_1$. According to Lemma 1, $R(p_l)R^T(p_l)$ is invertible for $(\tilde{p}_l(t), v_l(t)) \in \mathcal{T}_1$.

Substituting (33) and (36) into (35) yields

$$\dot{M}_2 = -k_v \beta^T(e_l) R(p_l) R^T(p_l) \beta(e_l) - k_a s_l^T s_l \quad (44)$$

therefore

$$\dot{M}_2 \leq -k_v \lambda_{\min}\left(R(p_l)R^T(p_l)\right) L(e_l) - k_a s_l^T s_l \quad \text{for } (\tilde{p}_l(t), v(t)) \in \mathcal{T}_1. \quad (45)$$

It follows from the negative definiteness of (44) that the level sets of M_2 are invariant [39] for $(\tilde{p}_l(0), v_l(0)) \in \mathcal{T}_1$ and therefore $(e_l, s_l) = 0$ is asymptotically stable for $(\tilde{p}_l(0), v_l(0)) \in \mathcal{T}_1$. Therefore, $\|p_{l_i}(t) - p_{l_j}(t)\| \to d_{l_{ij}}$ as $t \to \infty$ for all $(i, j) \in E_l$ and the control law (36) achieves the local asymptotic stability of the desired formation $F_l^* = (G_l^*, p_l^*)$. ■

Note that the condition (43) provides a set of allowed initial conditions $(\tilde{p}_l(0), v_l(0)) \in \mathcal{T}_1$ that will ensure the system stability.

Remark 6: The infinitesimal rigidity characteristic of the layered formation framework F_l ensures collision avoidance between all the connected agents i and j at any time $t > 0$.

The following lemma uses the absolute initial and desired positions of the agents and shows that (36) achieves the local asymptotic stability of the desired formation F_l^*. Therefore, Lemma 4 establishes the conditions that prevent convergence to ambiguous formations.

Lemma 4: Given model $\mathcal{W}_2$, let δ be a small positive constant and $p_l(0) \in \mathbb{R}^{3(n+r)}$ and $v_l(0) \in \mathbb{R}^{3(n+r)}$ are the initial conditions. Given $\Delta(G_l^*)$ being the maximum degree of the graph G_l^*, if $(p_l(0), v_l(0)) \in \mathcal{T}_2$ where

$$\mathcal{T}_2 = \Bigg\{ (p_l, v_l) \in \mathbb{R}^{3(n+r)} \times \mathbb{R}^{3(n+r)} \Bigg| 8|E_l| \max_{i \in V_l} \left\|p_{l_i} - p_{l_i}^*\right\|^2 \left(\left\|p_{l_i} - p_{l_i}^*\right\| + D_l\right)^2 + |V_l| \left(\max_{i \in V_l} \left\|v_{l_i}\right\| + \Delta\left(G_l^*\right) k_v \left(2 \max_{i \in V_l} \left\|p_{l_i} - p_{l_i}^*\right\| + D_l \right)^3 \right)^2 \leq 2\delta \Bigg\} \quad (46)$$

then $F_l(t)$ is infinitesimally and minimally rigid and the control law (36) achieves the asymptotic stability of the desired formation F_l^* and ensures $\|p_{l_i}(t) - p_{l_j}(t)\| \to d_{l_{ij}}$ as $t \to \infty$ for all $(i, j) \in E_l$.

Proof: Using (25), the sufficient condition for (41) is given by

$$\frac{1}{2}|E_l| \left(\max_{(i,j)\in E_l} \left(\left\|p_{l_i} - p_{l_i}^*\right\| + \left\|p_{l_j} - p_{l_j}^*\right\| \right)^2 \max_{(i,j)\in E_l} \left(\left\|p_{l_i} - p_{l_i}^*\right\| + \left\|p_{l_j} - p_{l_j}^*\right\| + 2d_{l_{ij}} \right)^2 \right) + |V_l| \max_{i \in V_l} \left\| v_{l_i} + k_v \sum_{j \in \Psi_i} \tilde{p}_{l_{ij}} e_{l_{ij}} \left(e_{l_{ij}} + 2d_{l_{ij}}\right) \right\|^2 \leq 2\delta. \quad (47)$$

$$8|E_l| \max_{i \in V_l} \left\|p_{l_i} - p_{l_i}^*\right\|^2 \left(\left\|p_{l_i} - p_{l_i}^*\right\| + D_l\right)^2 + |V_l| \max_{i \in V_l} \left\| v_{l_i} + k_v \sum_{j \in \Psi_i} \tilde{p}_{l_{ij}} e_{l_{ij}} \left(e_{l_{ij}} + 2d_{l_{ij}}\right) \right\|^2 \leq 2\delta. \quad (48)$$

This article has been accepted for inclusion in a future issue of this journal. Content is final as presented, with the exception of pagination.

Using the triangle inequality, the sufficient condition is given by

$$8|E_l| \max_{i\in V_l} \|p_{l_i} - p^*_{l_i}\|^2 \left(\|p_{l_i} - p^*_{l_i}\| + D_l\right)^2 + |V_l| \max_{i\in V_l} \left(\|v_{l_i}\| + k_v \sum_{j\in\Psi_i} \|\tilde{p}_{l_{ij}}\|^3 \right)^2 \leq 2\delta. \tag{49}$$

$$8|E_l| \max_{i\in V_l} \|p_{l_i} - p^*_{l_i}\|^2 \left(\|p_{l_i} - p^*_{l_i}\| + D_l\right)^2 + |V_l| \max_{i\in V_l} \left(\|v_{l_i}\| + k_v \sum_{j\in\Psi_i} \left(\|p_{l_i} - p^*_{l_i}\| + \left\|p_{l_j} - p^*_{l_j}\right\| + d_{l_{ij}} \right)^3 \right)^2 \leq 2\delta. \tag{50}$$

A sufficient condition for (50) is given by

$$8|E_l| \max_{i\in V_l} \|p_{l_i} - p^*_{l_i}\|^2 \left(\|p_{l_i} - p^*_{l_i}\| + D_l\right)^2 + |V_l| \left(\max_{i\in V_l} \|v_{l_i}\| + \Delta(G^*_l) k_v \left(2 \max_{i\in V_l} \|p_{l_i} - p^*_{l_i}\| + D_l \right)^3 \right)^2 \leq 2\delta. \tag{51}$$

Using Theorem 4, it follows that $\|p_{l_i}(t) - p_{l_j}(t)\| \rightarrow d_{l_{ij}}$ as $t \rightarrow \infty$ for all $(i, j) \in E_l$ and the control law (36) achieves the local asymptotic stability of the desired formation $F^*_l = (G^*_l, p^*_l)$. ■

Remark 7: The set (46) specifies allowed initial conditions in terms of positions and velocities of mobile agents. It is a balanced tradeoff between large initial velocity and large initial position errors. For example, for zero initial velocities, the condition sets an upper bound on initial position errors that ensures the system stability.

V. Simulation Results

A set of simulations was performed to demonstrate the performance of the proposed method for solving the layered formation control problem.

A. Single Integrator Model

In this section, we demonstrate the performance of the control law in (15) for a 3-D case (the upper layer agents are outside of the plane where the lower layer agents operate).

The following initial conditions were chosen for the agents:

$$p_{l_i}(0) = p^*_{l_i} + \alpha I_1, i = 1, \ldots, n, n+1, \ldots, n+r \tag{52}$$

where α is a uniform random number on the interval (0, 1) and I_1 generates a 3×1 unit vector of uniformly distributed random values on the interval $(0, 2\pi)$. In the simulations, the value of k_c was set to 1 in (15).

The simulation was conducted using six lower layer agents and one upper layer agent. The desired formation of the agents that was chosen for this simulation is shown in Fig. 4 where vertices 1 through 6 represent the six lower layer agents and vertex 7 represents the upper layer agent. This simulation scenario can emulate, for instance, a formation of UUVs that move underwater and a supervising ship that moves on the surface of water.

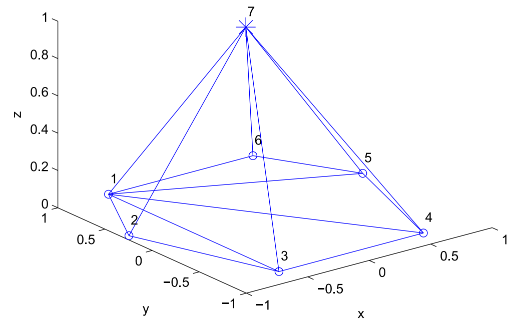

Fig. 4. Desired formation for six lower layer agents (circles) and one upper layer agent (star).

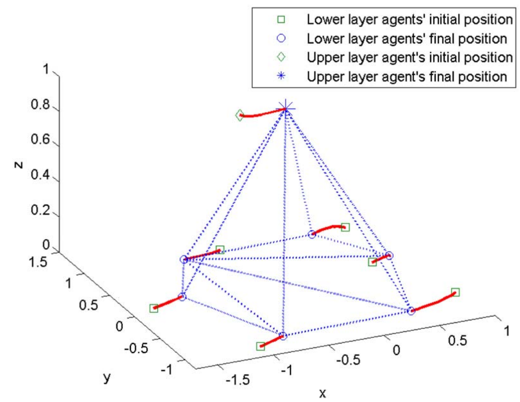

Fig. 5. Agents' trajectories $p_{l_i}(t)$, $i = 1, \ldots, 7$ with single integrator model (solid line) and desired formation (dotted line).

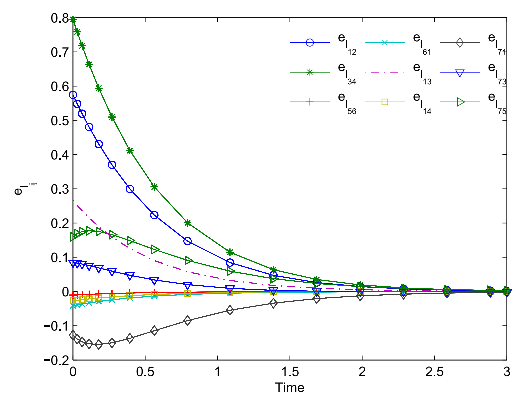

Fig. 6. Sample of distance errors for six lower layer agents and the upper layer agent.

The desired layered framework was chosen in the shape of a cone that is infinitesimally and minimally rigid (see Fig. 4).

Fig. 5 shows the trajectories for the six lower layer agents and the upper layer agent as they move from their initial position to the final position to form the desired layered formation. Fig. 6 demonstrates the distance errors $e_{l_{ij}}$ approaching zero. The control input $u_{l_i}(t)$ for $i = 1, \ldots, 7$ in the x and y directions are shown in Figs. 7 and 8, respectively.

This article has been accepted for inclusion in a future issue of this journal. Content is final as presented, with the exception of pagination.

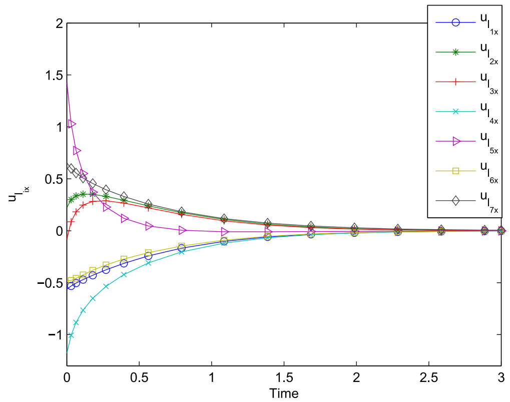

Fig. 7. Control inputs $u_{l_{ix}}(t)$, $i = 1, \ldots, 7$ in the x-direction.

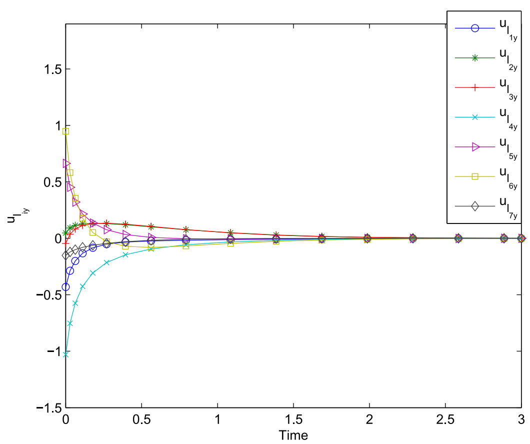

Fig. 8. Control inputs $u_{l_{iy}}(t)$, $i = 1, \ldots, 7$ in the y-direction.

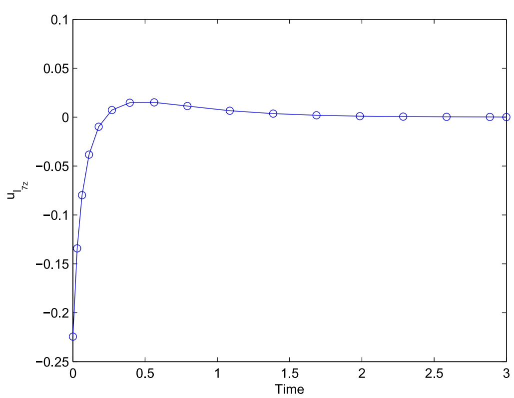

Fig. 9. Control input in the z-direction for the upper layer agent.

Fig. 9 shows the control input $u_{l_i}(t)$ for only $i = 7$ in the z-direction since the location of the other agents is defined by $p_{l_i} = (x_{l_i}, y_{l_i}, 0) \in \mathbb{R}^3$.

B. Double Integrator Model

The simulations in this section were performed for the scenario with five lower layer agents and three upper layer agents using the proposed control law (36).

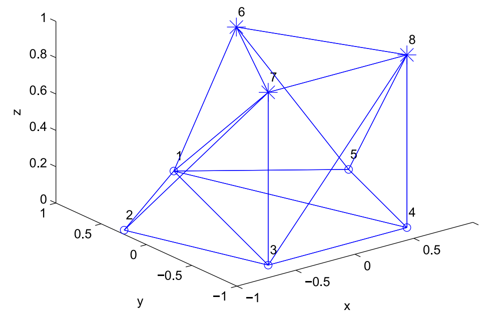

Fig. 10. Desired formation for five lower layer agents and three upper layer agents with double integrator model.

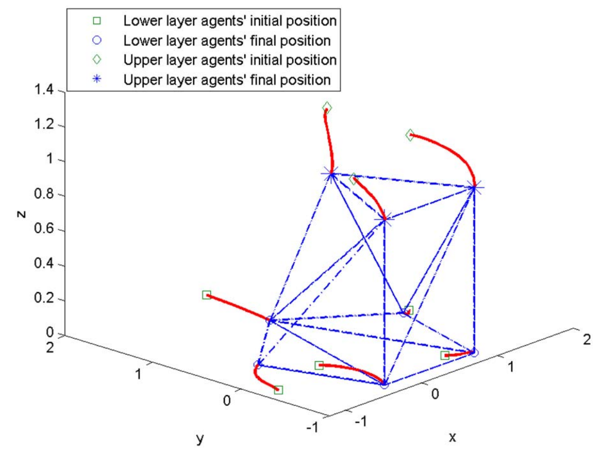

Fig. 11. Agents' trajectories $p_{l_i}(t)$, $i = 1, \ldots, 8$ with double integrator model (solid line) and desired formation (dotted line).

The initial conditions that were chosen for the agents were (52) and

$$v_{l_i}(0) = \alpha - 0.5I_2, i = 1, \ldots, n, n+1, \ldots, n+r \quad (53)$$

where I_2 generates a 3×1 unit vector of uniformly distributed random values on the interval (0, 1). The control gains k_a and k_v were set to 1 in (36).

The desired formation and trajectories of the agents as they move from the initial position to the final position are shown in Figs. 10 and 11, respectively. This simulation case can emulate a battlefield scenario where multiple UGVs move in a formation on the ground and multiple UAVs supervise them at a certain altitude, while providing intelligence and situational awareness to the UGVs for performing a mission.

Fig. 12 shows the distance errors $e_{l_{ij}}$ approaching zero. The control input $u_{l_i}(t)$ for $i = 1, \ldots, 8$ in the x and y directions are presented in Figs. 13 and 14 and $u_{l_i}(t)$ for $i = 6, 7, 8$ in the z-direction is shown in Fig. 15.

C. Vehicle Dynamics

Here, we present the simulation results for the layered formation of multiple robotic vehicles and one upper layer agent. We use the dynamics of a class of robotic vehicles (includes wheeled mobile robots, underwater vehicles with constant depth, aircraft with constant altitude, and marine vessels) that

This article has been accepted for inclusion in a future issue of this journal. Content is final as presented, with the exception of pagination.

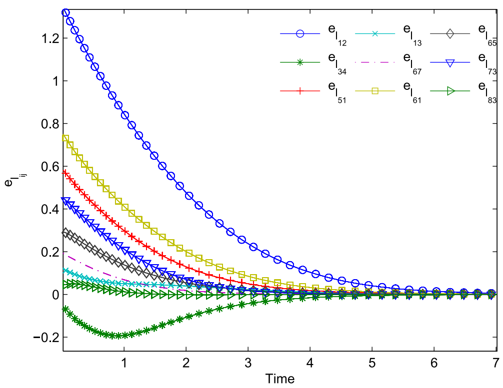

Fig. 12. Sample of distance errors for five lower layer agents and three upper layer agents.

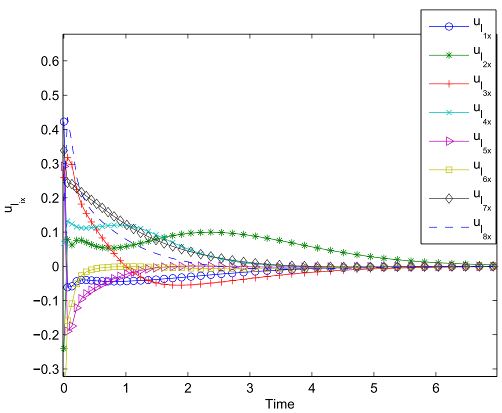

Fig. 13. Control inputs $u_{l_{ix}}(t)$, $i = 1, \ldots, 8$ in the x-direction.

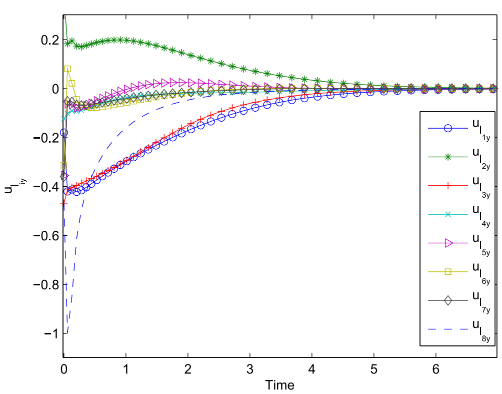

Fig. 14. Control inputs $u_{l_{iy}}(t)$, $i = 1, \ldots, 8$ in the y-direction.

is given by the following model [8]:

$$\begin{cases} \dot{q}_l = \omega_l \\ J_l(q_l)\ \dot{\omega}_l = \bar{u}_l - C_l(q_l, \dot{q}_l)\ \omega_l - H_l(q)\ \omega_l \end{cases} \tag{54}$$

where $q_l = (x_l, y_l) \in \mathbb{R}^2$ is the hand position of the robotic vehicle with respect to an earth-fixed coordinate frame, $\omega_l \in \mathbb{R}^2$ is the velocity of the vehicles relative to an Earth-fixed frame, $\bar{u}_l \in \mathbb{R}^2$ represents the force/torque level control input and is given in (36), $J_l(q_l) \in \mathbb{R}^{2n\times 2n}$ is the mass matrix, $C_l(q_l, \dot{q}_l) \in \mathbb{R}^{2n\times 2n}$ is the Coriolis matrix, and $H_l(q_l) \in \mathbb{R}^{2n\times 2n}$ is the damping matrix. The dynamic model of a mobile robot can be feedback linearized if the orientation of the robot

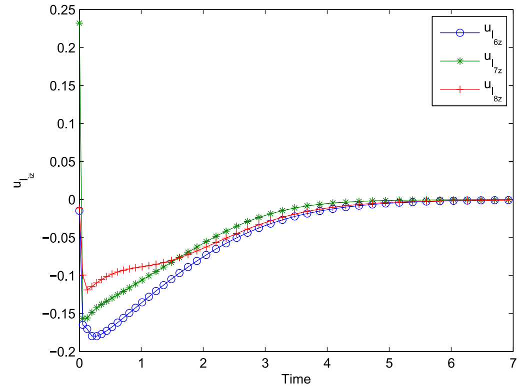

Fig. 15. Control inputs in the z-direction for the upper layer agents.

is ignored and the control is focused on an off-wheel axis point on the mobile robot, called robot hand point [42]. More precisely, the robot hand point q_l is defined as a point that is located at a distance L from the center of mass of robot and on the robot's orientation axis.

The expressions for the matrices $J_l(q_l)$, $C_l(q_l, \dot{q}_l)$, and $H_l(q_l)$ are given in the Appendix and the derivation of these matrices can be found in [8]. The model used for the upper layer agent was the same as in Section V-B.

In this simulation, there are four robotic vehicles and one upper layer agent. The initial positions of the robotic vehicles were set to

$$q_{l_i}(0) = q^*_{l_i} + \alpha I_3,\ i = 1, \ldots, 4 \tag{55}$$

where $q^*_{l_i}$ is the desired position of the agents and I_3 generates a 2×1 unit vector of uniformly distributed random values on the interval $(0, 2\pi)$. The initial orientations and velocities of the vehicles were chosen as

$$\theta_{l_i}(0) = \sigma_1 I_4,\ i = 1, \ldots, 4 \tag{56}$$

$$\omega_{l_i}(0) = \sigma_2[I_5 - 0.5],\ i = 1, \ldots, 4 \tag{57}$$

where $\sigma_1 = 1$, I_4 is a uniformly distributed random number on the interval $(0, 1)$, $\sigma_2 = 2\pi$, and I_5 generates a 2×1 unit vector of uniformly distributed values on the interval $(0, 1)$. The parameters such as mass and moment of inertia of the vehicles that are used in matrices $J_l(q_l)$ and $C_l(q_l, \dot{q}_l)$ were set to $m = 4$ kg and $I = 0.0405$ kg m^2, respectively. The distance between the center of mass of the vehicle and the hand position was chosen as $L = 0.15$ m. The constant damping matrix $\bar{H}_{l_i} = \text{diag}(0.4 \text{ kg/s}, 0.005 \text{ kg m}^2\text{/s})$ for $i = 1, \ldots, n$ was chosen for the simulation.

The initial position of the upper layer agent was chosen as (52) and its velocity was set to

$$\omega_{l_5}(0) = \sigma_2[I_2 - 0.5]. \tag{58}$$

The control gains k_a and k_v in (36) were set to 20 and 1, respectively.

An infinitesimally and minimally rigid formation, shown with dotted lines in Fig. 16, with nine communication/control links was chosen as the desired formation. Fig. 16 shows the trajectories of the agents, as they move from their initial positions to the final positions and get into the desired formation. Fig. 17 shows the distance errors $e_{l_{ij}}$ approaching zero.

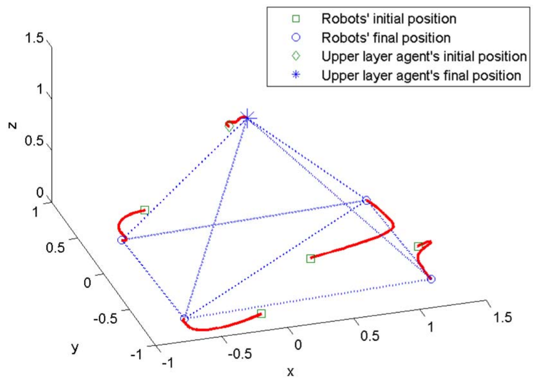

Fig. 16. Agents' trajectories $q_{l_i}(t)$, $i = 1, \ldots, 5$ (solid line) and desired formation (dotted line).

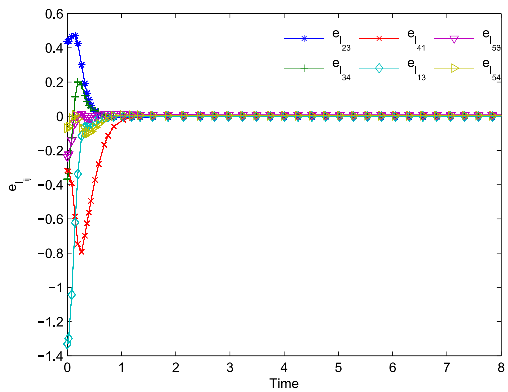

Fig. 17. Sample of distance errors (m) versus time (s) for four robotic vehicles and one upper layer agent.

From these simulation examples, it can be seen that distance errors converge to zero with time. Notice that in the case of vehicle dynamics, the error converges to the small bounded neighborhood of zero. That is to be expected since the robotic vehicle dynamics is not an ideal integrator model, rather a dynamic model with extra terms.

VI. Conclusion

In this paper, we considered the problem of formation acquisition for a group of n agents that belong to a plane Q and r agents that move in an upper layer outside of the plane Q. Graph coning and triangulation concepts were used to create a 3-D framework that retains the infinitesimal and minimal rigidity characteristics of the framework of n lower layer agents. By using the proposed approach, the interagent distances were stabilized to acquire a predefined shape in 3-D. Sufficient conditions were provided for the initial conditions that guarantee convergence of the layered formation to the desired framework. The simulation results showed that the proposed control method, using single and double integrator models, yields asymptotic stability of the desired formation. As future work, the application of robust and intelligent control techniques within the proposed framework as well as the real time implementation of the proposed method will be investigated.

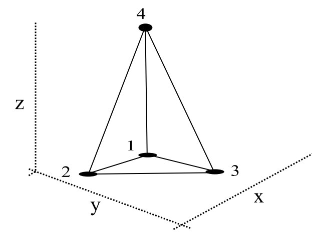

Fig. 18. Infinitesimally and minimally rigid graph in 3-D.

Appendix A

An undirected infinitesimally and minimally rigid graph $G = (V, E)$ in 3-D is shown in Fig. 18. The corresponding rigidity matrix $R(p)$ is given in (59) where $\tilde{p}_{ij}^T = [x_i - x_j, y_i - y_j, z_i - z_j]$ and each $\mathbf{0}$ is a 1×3 vector of zeroes.

$$R(p) = \begin{bmatrix} \tilde{p}_{12}^T & \tilde{p}_{21}^T & \mathbf{0} & \mathbf{0} \\ \mathbf{0} & \tilde{p}_{23}^T & \tilde{p}_{32}^T & \mathbf{0} \\ \tilde{p}_{13}^T & \mathbf{0} & \tilde{p}_{31}^T & \mathbf{0} \\ \tilde{p}_{14}^T & \mathbf{0} & \mathbf{0} & \tilde{p}_{41}^T \\ \mathbf{0} & \tilde{p}_{24}^T & \mathbf{0} & \tilde{p}_{42}^T \\ \mathbf{0} & \mathbf{0} & \tilde{p}_{34}^T & \tilde{p}_{43}^T \end{bmatrix}. \tag{59}$$

Appendix B

The mass matrix in (54) is given by $J_l(q_l) = \operatorname{diag}(J_{l_i}(q_{l_i}))$ for $i = 1, \ldots, n$. The term $J_{l_i}(q_{l_i})$ is defined as $J_{l_i}(q_{l_i}) = \eta^T \bar{J}_l \eta$ where $\bar{J}_l = \operatorname{diag}(m, I)$ and

$$\eta(\theta_{l_i}) = \begin{bmatrix} \cos\theta_{l_i} & \sin\theta_{l_i} \\ -\frac{\sin\theta_{l_i}}{L} & \frac{\cos\theta_{l_i}}{L} \end{bmatrix} \tag{60}$$

$$J_{l_i}(q_{l_i}) = \begin{bmatrix} J_{l_{11}} & J_{l_{12}} \\ J_{l_{21}} & J_{l_{22}} \end{bmatrix} \tag{61}$$

$$J_{l_{11}} = m\cos^2(\theta_{l_i}) + \frac{I}{L^2}\sin^2(\theta_{l_i})$$

$$J_{l_{12}} = \left(m - \frac{I}{L^2}\right)\cos\theta_{l_i}\sin\theta_{l_i}$$

$$J_{l_{21}} = \left(m - \frac{I}{L^2}\right)\cos\theta_{l_i}\sin\theta_{l_i}$$

$$J_{l_{22}} = m\sin^2(\theta_{l_i}) + \frac{I}{L^2}\cos^2(\theta_{l_i}).$$

The Coriolis matrix is given by $C_l(q_l, \dot{q}_l) = \operatorname{diag}(C_{l_i}(q_{l_i}, \dot{q}_{l_i}))$ for $i = 1, \ldots, n$. The term $C_{l_i}(q_{l_i}, \dot{q}_{l_i})$ is defined as $C_{l_i}(q_{l_i}, \dot{q}_{l_i}) = \eta^T \bar{J}_l \dot{\eta}$ and is given by

$$C_{l_i}(q_{l_i}, \dot{q}_{l_i}) = \begin{bmatrix} C_{l_{11}} & C_{l_{12}} \\ C_{l_{21}} & C_{l_{22}} \end{bmatrix} \tag{62}$$

$$C_{l_{11}} = -\left(m - \frac{I}{L^2}\right)\dot{\theta}_{l_i}\cos(\theta_{l_i})\sin(\theta_{l_i})$$

$$C_{l_{12}} = m\,\dot{\theta}_{l_i}\cos^2(\theta_{l_i}) + \frac{I}{L^2}\dot{\theta}_{l_i}\sin^2(\theta_{l_i})$$

$$C_{l_{21}} = -m\,\dot{\theta}_{l_i}\sin^2(\theta_{l_i}) - \frac{I}{L^2}\dot{\theta}_{l_i}\cos^2(\theta_{l_i})$$

$$C_{l_{22}} = \left(m - \frac{I}{L^2}\right)\dot{\theta}_{l_i}\cos(\theta_{l_i})\sin(\theta_{l_i}).$$

The damping matrix is given by $H_l(q_l) = \operatorname{diag}(H_{l_i}(q_{l_i}))$ for $i = 1, \ldots, n$. The term $H_{l_i}(q_{l_i})$ is defined as $H_{l_i}(q_{l_i}) = \eta^T \bar{H}_{l_i}\eta$.

REFERENCES

[1] X. Cai and M. de Queiroz, "Multi-agent formation maintenance and target tracking," in *Proc. Amer. Control Conf. (ACC)*, Washington, DC, USA, Jun. 2013, pp. 2521–2526.

[2] B. D. O. Anderson, C. Yu, B. Fidan, and J. Hendrickx, "Rigid graph control architectures for autonomous formations," *IEEE Control Syst.*, vol. 28, no. 6, pp. 48–63, Dec. 2008.

[3] D. J. Pack, P. DeLima, G. J. Toussaint, and G. York, "Cooperative control of UAVs for localization of intermittently emitting mobile targets," *IEEE Trans. Syst., Man, Cybern. B, Cybern.*, vol. 39, no. 4, pp. 959–970, Aug. 2009.

[4] S. Ramazani, D. L. Jackson, and R. R. Selmic, "Cooperative mobile agents search using beehive partitioned structure and tabu random search algorithm," in *Proc. 15th SPIE Unmanned Syst. Technol.*, 2013, Art. no. 874108.

[5] B. D. O. Anderson, C. Yu, S. Dasgupta, and A. S. Morse, "Control of a three-coleader formation in the plane," *Syst. Control Lett.*, vol. 56, nos. 9–10, pp. 573–578, 2007.

[6] L. Asimow and B. Roth, "The rigidity of graphs, II," *J. Math. Anal. Appl.*, vol. 68, no. 1, pp. 171–190, Mar. 1979.

[7] T.-S. Tay and W. Whiteley, "Generating isostatic frameworks," *Struct. Topol.*, vol. 11, pp. 21–69, 1985.

[8] X. Cai and M. de Queiroz, "Adaptive rigidity-based formation control for multirobotic vehicles with dynamics," *IEEE Trans. Control Syst. Technol.*, vol. 23, no. 1, pp. 389–396, Jan. 2015.

[9] K.-K. Oh and H.-S. Ahn, "Distance-based undirected formations of single-integrator and double-integrator modeled agents in *n*-dimensional space," *Int. J. Robust Nonlin. Control*, vol. 24, no. 12, pp. 1809–1820, 2014.

[10] K.-K. Oh and H.-S. Ahn, "Distance-based control of cycle-free persistent formations," in *Proc. IEEE Int. Symp. Intell. Control (ISIC)*, Denver, CO, USA, Sep. 2011, pp. 816–821.

[11] K.-K. Oh, M.-C. Park, and H.-S. Ahn, "A survey of multi-agent formation control," *Automatica*, vol. 53, pp. 424–440, Mar. 2015.

[12] T. H. Summers, C. Yu, S. Dasgupta, and B. D. O. Anderson, "Control of minimally persistent leader-remote-follower and coleader formations in the plane," *IEEE Trans. Autom. Control*, vol. 56, no. 12, pp. 2778–2792, Dec. 2011.

[13] K.-K. Oh and H.-S. Ahn, "Formation control of mobile agents based on inter-agent distance dynamics," *Automatica*, vol. 47, no. 10, pp. 2306–2312, 2011.

[14] L. Krick, M. E. Broucke, and B. A. Francis, "Stabilization of infinitesimally rigid formations of multi-robot networks," in *Proc. 47th IEEE Conf. Decis. Control (CDC)*, Cancún, Mexico, 2008, pp. 477–482.

[15] S.-M. Kang, M.-C. Park, B.-H. Lee, and H.-S. Ahn, "Distance-based formation control with a single moving leader," in *Proc. Amer. Control Conf. (ACC)*, Portland, OR, USA, Jun. 2014, pp. 305–310.

[16] M.-C. Park, K. Jeong, and H.-S. Ahn, "Formation stabilization and resizing based on the control of inter-agent distances," *Int. J. Robust Nonlin. Control*, vol. 25, no. 14, pp. 2532–2546, 2015.

[17] M. Aranda, G. López-Nicolás, C. Sagüés, and M. M. Zavlanos, "Coordinate-free formation stabilization based on relative position measurements," *Automatica*, vol. 57, pp. 11–20, Jul. 2015.

[18] D. Jin and L. Gao, "Stability analysis of a double integrator swarm model related to position and velocity," *Trans. Inst. Measur. Control*, vol. 30, nos. 3–4, pp. 275–293, 2008.

[19] M.-C. Park, Z. Sun, B. D. O. Anderson, and H.-S. Ahn, "Stability analysis on four agent tetrahedral formations," in *Proc. IEEE 53rd Annu. Conf. Decis. Control (CDC)*, Los Angeles, CA, USA, 2014, pp. 631–636.

[20] X. Cai and M. de Queiroz, "Rigidity-based stabilization of multi-agent formations," *ASME J. Dyn. Syst. Measur. Control*, vol. 136, no. 1, Jan. 2014, Art. no. 014502.

[21] B. D. O. Anderson, B. Fidan, C. Yu, and D. Walle, "UAV formation control: Theory and application," in *Recent Advances in Learning and Control* (Lecture Notes in Control and Information Sciences), vol. 371. London, U.K.: Springer, 2008, pp. 15–33.

[22] M. Bryant, P. Johnson, B. M. Kent, M. Nowak, and S. Rogers, "Layered sensing," White Paper Version 6, Air Force Res. Lab., Rome, NY, USA, May 2008.

[23] W. Whiteley, "Cones, infinity and 1-story buildings," *Struct. Topol.*, vol. 8, pp. 53–70, 1983.

[24] R. Connelly and W. J. Whiteley, "Global rigidity: The effect of coning," *Discr. Comput. Geom.*, vol. 43, no. 4, pp. 717–735, 2010.

[25] B. Jackson and T. Jordán, "Connected rigidity matroids and unique realizations of graphs," *J. Comb. Theory B*, vol. 94, no. 1, pp. 1–29, 2005.

[26] G. Laman, "On graphs and rigidity of plane skeletal structures," *J. Eng. Math.*, vol. 4, no. 4, pp. 331–340, 1970.

[27] C. Yu, B. D. O. Anderson, S. Dasgupta, and B. Fidan, "Control of minimally persistent formations in the plane," *SIAM J. Control Optim.*, vol. 48, no. 1, pp. 206–233, 2009.

[28] W. Whiteley, "Some matroids from discrete applied geometry," *Contemp. Math.*, vol. 197, pp. 171–311, 1996.

[29] H. Maehara, "Geometry of frameworks," *Yokohama Math. J.*, vol. 47, pp. 41–65, 1999.

[30] R. Connelly, "Generic global rigidity," *Discr. Comput. Geom.*, vol. 33, no. 4, pp. 549–563, Apr. 2005.

[31] R. Connelly, "The rigidity of polyhedral surfaces," *Math. Mag.*, vol. 52, no. 5, pp. 275–283, Nov. 1979.

[32] L. Asimow and B. Roth, "The rigidity of graphs," *Trans. Amer. Math. Soc.*, vol. 245, pp. 279–289, Nov. 1978.

[33] R. Connelly, "The rigidity of certain cabled frameworks and the second-order rigidity of arbitrarily triangulated convex surfaces," *Adv. Math.*, vol. 37, no. 3, pp. 272–299, 1980.

[34] J. F. Roberts, T. Stirling, J.-C. Zufferey, and D. Floreano, "3-D relative positioning sensor for indoor flying robots," *Auton. Robots*, vol. 33, nos. 1–2, pp. 5–20, 2012.

[35] F. Dörfler and B. Francis, "Geometric analysis of the formation problem for autonomous robots," *IEEE Trans. Autom. Control*, vol. 55, no. 10, pp. 2379–2384, Oct. 2010.

[36] R. Olfati-Saber and P. Jalalkamali, "Coupled distributed estimation and control for mobile sensor networks," *IEEE Trans. Autom. Control*, vol. 57, no. 10, pp. 2609–2614, Oct. 2012.

[37] J. Qin, W. X. Zheng, and H. Gao, "Coordination of multiple agents with double-integrator dynamics under generalized interaction topologies," *IEEE Trans. Syst., Man, Cybern. B, Cybern.*, vol. 42, no. 1, pp. 44–57, Feb. 2012.

[38] H. Gluck, "Almost all simply connected closed surfaces are rigid," in *Geometric Topology*, vol. 438. Heidelberg, Germany: Springer, 1975, pp. 225–239.

[39] H. K. Khalil, *Nonlinear Systems*. Upper Saddle River, NJ, USA: Prentice Hall, 2002.

[40] S. Ramazani, R. R. Selmic, and M. de Queiroz, "Non-planar multi-agent formation control using coning graphs," in *Proc. IEEE Int. Conf. Syst. Man Cybern. (SMC)*, San Diego, CA, USA, Oct. 2014, pp. 3091–3096.

[41] Y.-Y. Chen and Y.-P. Tian, "A backstepping design for directed formation control of three-coleader agents in the plane," *Int. J. Robust Nonlin. Control*, vol. 19, no. 7, pp. 729–745, 2009.

[42] Y. Zou, "Distributed control of multiple vehicle systems using constraint forces," Ph.D. dissertation, School Mech. Aerosp. Eng., Oklahoma State Univ. Stillwater, Stillwater, OK, USA, 2008.

Saba Ramazani (S'14) received the B.S. and M.S. degrees in electrical engineering from Louisiana Tech University, Ruston, LA, USA, in 2011 and 2013, respectively, where She is currently pursuing the Ph.D. degree in engineering with cyberspace concentration.

She is currently a NASA and Louisiana Space Consortium Research Fellow. Her current research interests include unmanned and multiagent systems, cooperative control, artificial neural networks, and control systems security.

Rastko Selmic (SM'08) received the B.S. degree from the University of Belgrade, Belgrade, Serbia, in 1994, and the M.S. and Ph.D. degrees from the University of Texas at Arlington, Arlington, TX, USA, in 1997 and 2000, respectively, all in electrical engineering.

He was a Lead DSP Systems Engineer with Signalogic Inc., Dallas, TX, USA, from 1997 to 2002. In 2002, he joined the Electrical Engineering Department, Louisiana Tech University, Ruston, LA, USA, where he is currently an AT& T Professor of Electrical Engineering. He was a Research Fellow with Air Force Research Laboratory, Dayton, OH, USA, from 2007 to 2008 and in 2015. He has author/co-authored 70 journal and conference papers, four book chapters, and the book entitled *Neuro-Fuzzy Control of Industrial Systems With Actuator Nonlinearities* (SIAM Press, 2002). He holds one U.S. patent with four additional reports of invention. He consulted for numerous companies, including Andrew Corporation, Richardson, TX, USA, Intelligent Automation Inc., Rockville, MD, USA, Davis Technologies International Inc., Dallas, and American GNC Corporation, Simi Valley, CA, USA. His current research interests include smart sensors and actuators, cooperative sensing and control, gesture-based computing and control, and UAV control.

Dr. Selmic served as an Associate Editor for the IEEE TRANSACTIONS ON NEURAL NETWORKS and currently serves as an Associate Editor for the IEEE TRANSACTIONS ON CYBERNETICS. He is a Senior Member of Sigma Xi.

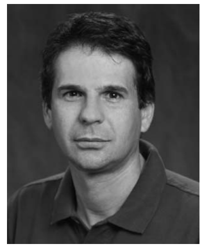

Marcio de Queiroz (M'94) received the B.S. degree in electrical engineering from the Federal University of Rio de Janeiro, Rio de Janeiro, Brazil, the M.S. degree in mechanical engineering from the Pontifical Catholic University of Rio de Janeiro, Rio de Janeiro, and the Ph.D. degree in electrical engineering from Clemson University, Clemson, SC, USA, in 1997.

From 1997 to 1998, he was a Post-Doctoral Researcher with the Rotating Machinery and Controls Laboratories, University of Virginia, Charlottesville, VA, USA. From 1998 to 2000, he was a Visiting Assistant Professor with the Department of Mechanical Engineering, NYU Tandon School of Engineering, Brooklyn, NY, USA. In 2000, he joined the Department of Mechanical and Industrial Engineering, Louisiana State University, Baton Rouge, LA, USA, where he is currently the Roy O. Martin Lumber Company Professor. His current research interests include nonlinear control theory and applications, multiagent systems, robotics, active magnetic and mechanical bearings, and biological/biomedical system modeling and control.

Dr. de Queiroz was a recipient of the NSF CAREER Award in 2005. He served as an Associate Editor for the IEEE TRANSACTIONS ON AUTOMATIC CONTROL, the *ASME Journal of Dynamic Systems, Measurement, and Control*, the IEEE/ASME TRANSACTIONS ON MECHATRONICS, and the IEEE TRANSACTIONS ON SYSTEMS, MAN, AND CYBERNETICS—PART B: CYBERNETICS.